JOURNAL OF BACTERIOLOGY, Feb. 1995, p. 580–585
0021-9193/95/$04.00+0

Vol. 177, No. 3

Characterization of Novel Yeast *RAD6* (*UBC2*) Ubiquitin-Conjugating Enzyme Mutants Constructed by Charge-to-Alanine Scanning Mutagenesis

MICHELE MCDONOUGH,† PITCHAI SANGAN, AND DAVID K. GONDA*

Department of Molecular Biophysics and Biochemistry, Yale University School of Medicine, New Haven, Connecticut 06520-8024

Received 19 September 1994/Accepted 16 November 1994

Ubiquitination of intracellular proteins by the yeast *RAD6* (*UBC2*) ubiquitin-conjugating (E2) enzyme is required for cellular processes as diverse as DNA repair, selective proteolysis, and normal growth. For most *RAD6*-dependent functions, the relevant in vivo targets, as well as the mechanisms and cofactors that govern *RAD6* substrate selectivity, are unknown. We have explored the utility of "charge-to-alanine" scanning mutagenesis to generate novel *RAD6* mutants that are enzymatically competent with respect to unfacilitated (E3-independent) ubiquitination but that are nevertheless severely handicapped with respect to several in vivo functions. Five of the nine mutants we generated show defects in their in vivo functions, but almost all of the most severely affected mutants displayed unfacilitated ubiquitin-conjugating activity in vitro. We suggest that E2 mutants obtained by this approach are likely to be defective with respect to interaction with other, *trans*-acting factors required for their intracellular activity or substrate selectivity and therefore will be useful for further genetic and biochemical studies of ubiquitin-conjugating enzyme function.

Covalent attachment of the highly conserved protein ubiquitin to other eucaryotic proteins is required for many cellular functions including stress resistance, selective proteolysis of most normal and abnormal short-lived proteins, cell cycle progression, and DNA repair (11, 17, 21). Ubiquitination of proteins is catalyzed by an elaborate multienzyme conjugation pathway whose components are conserved in eucaryotes (21). The first step in the ubiquitin ligation pathway is the ATP-dependent activation of ubiquitin via the formation of a thioester between the ubiquitin C terminus and a cysteine residue in ubiquitin-activating (E1) enzyme. Ubiquitin is then transferred from the E1 to one of several ubiquitin-conjugating (E2) enzymes, also via a thioester formed with a conserved Cys residue. Finally, ubiquitin is transferred from the E2 to a protein substrate in a reaction that often requires a third factor, called a ubiquitin protein ligase or E3 (11, 17, 21).

The yeast *Saccharomyces cerevisiae* has provided a genetically tractable system for studies of ubiquitin-dependent pathways (14, 23). The first E2 to be cloned was that encoded by the yeast *RAD6* (*UBC2*) gene (22). Mutations in *RAD6* are pleiotropic: among the phenotypes displayed are sensitivity to DNA-damaging agents and a defect in postreplication repair of DNA (30), deficiency in UV-induced mutagenesis (26), altered integration site preference for retrotransposition (27), absence of selective proteolysis via the N-end rule pathway (8, 38), a general growth deficiency and a temperature-sensitive cell cycle arrest (10), and (in homozygous *rad6*/*rad6* diploids) failure to sporulate (31). A *rad6* mutant allele lacking its single, active-site Cys yields the same array of phenotypes as a *rad6* null mutant (36, 37). Thus, the ubiquitin-conjugating activity of the RAD6 protein is required for its many in vivo functions.

Since the initial identification of *RAD6* as a ubiquitin-conjugating enzyme, more than 10 E2s have been cloned from *S. cerevisiae* (21). Mutations in different E2s yield strikingly different phenotypes, and many of the E2s appear to target distinct subsets of intracellular proteins for ubiquitination. However, relatively little is known about how their ubiquitin-conjugating activities are targeted to specific substrates. E3 proteins (when they are required) appear to govern substrate selectivity through formation of a complex with an E2 and a substrate (16, 18, 19, 32). Thus, the *UBR1*-encoded yeast E3 that governs substrate selection by the *RAD6*-dependent N-end rule proteolytic pathway forms a stable complex with *RAD6* and simultaneously binds target proteins that have a destabilizing amino-terminal residue (6, 8, 28, 34). Other *RAD6*-dependent functions may also require E3 proteins for substrate selection, though no putative homologs of UBR1 have been identified. Associated factors may play other roles in regulating E2 activity and E2-dependent functions. The RAD18 protein, which is encoded by another member of the *RAD6* epistasis group, also forms a complex with the RAD6 protein and may facilitate *RAD6*-dependent DNA repair by targeting the E2 to sites of damaged DNA (4).

It remains to be determined what structural determinants on an E2 specify its interaction with its substrates or with the *trans*-acting factors that govern activity and substrate selectivity. The RAD6 protein consists of a 150-residue N-terminal catalytic domain which is homologous to those found in other E2s, plus a 23-residue, aspartate-rich C-terminal domain (29). Madura et al. found that the acidic C-terminal domain is required for N-end rule pathway function in *S. cerevisiae* (but see reference 38 for a different view). It is also required for sporulation in diploids, but most other *RAD6*-dependent functions are provided by a truncation mutant that lacks the tail (28, 29). The first nine residues of *RAD6* have also been implicated in several *RAD6*-dependent functions; removal of those residues yields a mutant allele which is at least partly defective in most

* Corresponding author. Mailing address: Yale University School of Medicine, Department of Molecular Biophysics and Biochemistry, 333 Cedar St., P.O. Box 208024, SHM C-34, New Haven, CT 06520-8024. Phone: (203) 785-3321. Fax: (203) 785-6404. Electronic mail address: david_gonda@qm.yale.edu.

† Present address: Department of Molecular and Cellular Biology, State University of New York at Stony Brook, Stony Brook, NY 11794.

RAD6-dependent activities, including UV resistance, although the *rad6* N-terminal truncation mutant is still significantly more resistant to UV than a null mutant (38). However, this mutant still appears fully competent (if not more so) for UV-induced mutagenesis (38). Neither the C-terminal truncation mutant nor the N-terminal truncation mutant described above forms a tight complex with UBR1 as judged by coimmunoprecipitation experiments, thus explaining their defect with respect to UBR1-dependent proteolysis (4, 28).

RAD6 ubiquitinates some substrates (e.g., histones) in the absence of other factors such as E3 proteins (22, 35). We therefore reasoned that a *RAD6* mutant which still displays this E3-independent (unfacilitated) ubiquitin-conjugating activity, but which was no longer able to carry out specific in vivo (E3-dependent or -facilitated) functions, would be a candidate for a mutant allele that was specifically defective for interaction with regulators of *RAD6* activity or substrate specificity. Such mutants should be valuable reagents for biochemical and genetic studies directed towards understanding how *RAD6* activity is governed in vivo. We describe here experiments which explore the utility of using "charge-to-alanine" scanning mutagenesis to obtain such mutants. We report that this strategy (in which clusters of charged residues are targeted for mutagenesis to alanine) has yielded a number of novel N-terminal domain mutants of *RAD6* which appear to be enzymatically competent yet are defective with respect to several in vivo functions.

MATERIALS AND METHODS

Construction of yeast and *Escherichia coli* RAD6 expression vectors. All mutants were produced by PCR mutagenesis (20) using YCplac33RAD6 (25) as a template and subsequent subcloning between the *Sal*I and *Sph*I sites of (*URA3*-marked) YCplac33 (13). Descriptions of the oligonucleotides used in DNA constructions are available on request. The complete sequence of each mutated *RAD6* allele was verified by dideoxy-sequencing. Scan mutants were also subcloned between the *Sal*I and *Sph*I sites of (*TRP1*-marked) YCplac22 (13). Bacterial T7 vectors that express the *RAD6* scan mutants were made by subcloning the 0.6-kb *Eco*RI-*Eco*RI *RAD6* coding fragment from each mutant into the *Eco*RI site of pET-21(+) (Novagen). This T7 expression vector requires an insert-encoded ribosome binding site for protein expression, but the *Eco*RI-*Eco*RI fragment with the *RAD6* gene contains approximately 50 nucleotides upstream from the *RAD6* initiation codon, including sequences that have a cryptic bacterial ribosome binding site.

Yeast strains, growth, transformation, and microscopy. The strains used throughout this study were YMW1 (*MAT*α *ade2-1 ade3-22 his3-11,15 leu2-3,112 trp1-1 ura3-1 can1-100*) and YMW2 (*MAT***a** *ade2-1 ade3-22 his3-11,15 leu2-3,112 trp1-1 ura3-1 can1-100*; obtained from M. Solomon, and originally constructed by M. Wahlberg). To construct the *rad6*Δ::*LEU2* null tester strains, the *RAD6* loci of YMW1 and YMW2 were targeted by one-step gene disruption with a disruption module in which the *Eco*RI-*Eco*RI segment containing *RAD6* coding sequences had been replaced by *LEU2*; the resulting null mutant strains lacked all *RAD6* coding sequences. Yeast cells were propagated on yeast-peptone-dextrose (YPD), yeast-peptone-glycerol (YPglycerol), or synthetic complete (SC) media with appropriate selective omissions (1). Lithium acetate transformation of yeast cells was performed by a previously described method (33). To prevent propagation of respiratory petite mutations, tester strains were grown on YPglycerol plates prior to transformation and routinely tested for growth on YPglycerol.

Assay for temperature-sensitive growth. In addition to a general slow-growth phenotype, *rad6*Δ null mutants display a cell cycle arrest in late S or G_2 phase (10). To assay for this defect, YMW1*rad6*Δ::*LEU2* cells transformed with YCplac33 encoding *RAD6* scan mutants, a positive control (YCplac33RAD6), or a negative control (YCplac33) were grown in SC-Ura liquid media at 30°C overnight. The optical density at 600 nm (OD_{600}) of the cultures was measured, and cultures were diluted to a final OD_{600} of 1.0. A total of 200 μl of the diluted cultures was then prepared in the wells of a 96-well tissue culture plate, and samples of the cultures were transferred to multiple plates by stamping with a multipin inoculating manifold (a "frogger"). After being dried, the plates were incubated at the indicated temperature for up to several days and photographed. To test for the possibility of intra-allelic complementation of their temperature sensitivity defect, homozygous *rad6*Δ/*rad6*Δ diploids containing two independently encoded scan mutants were constructed as follows. Strain YMW1*rad6*Δ::*LEU2* transformed with a scan mutant in the (URA3-marked) vector YCplac33 was mated with strain YMW2*rad6*Δ::*LEU2* containing a scan mutant in the (TRP1-marked) vector YCplac22. Diploids were selected on SC-Ura-Trp media, and the diploid was tested as described above, except that cultures were stamped onto SC-Ura-Trp media. Recessiveness to wild-type *RAD6* of the scan mutants with respect to temperature-sensitive growth was performed either by doing the tests above with YCplac22-RAD6 (wild type) or by mating transformed YMW1*rad6*Δ::*LEU2* with YMW2 (*RAD6*$^+$).

Assay for sensitivity to UV irradiation. For testing of UV sensitivity, *S. cerevisiae* cells containing *RAD6* scan mutants were ponded onto plates as described above and then were exposed to germicidal UV (dosage, 0.5 J/m^2/s) at the indicated dosages. No strain grew with dosages of 150 J/m^2 or more (data not shown). Plates were immediately wrapped in foil and incubated at 30°C prior to photography. To test for intra-allelic complementation of their UV sensitivity defect, homozygous *rad6*Δ/*rad6*Δ diploids containing two independently encoded scan mutants were constructed as described for testing of temperature-sensitive growth above. The diploids were grown in SC-Ura-Trp media and assayed for sensitivity to UV as done for haploid *S. cerevisiae RAD6* scan mutants.

Assay for N-end rule pathway function. N-end rule pathway function was assayed by measuring the steady-state level of β-galactosidase (β-Gal) test proteins expressed in the strain being tested (2, 3, 5, 6, 15). The plasmid pLG-Ub-Met-βgal (all pLG plasmids described here are identical to those described by Bachmair et al. [2]) expresses a ubiquitin–Met–β-Gal fusion protein which is rapidly processed to yield free ubiquitin and Met–β-Gal. The resulting Met–β-Gal test protein has a half-life greater than 20 h and thus accumulates to a high steady-state level in cells. pLG-Ub-Arg-βgal expresses ubiquitin–Arg–β-Gal, which is similarly processed to produce free ubiquitin and Arg–β-Gal. However, because of the amino-terminal Arg, this test protein is very short lived and so accumulates to a much lower steady-state level (2); the degradation of Arg–β-Gal in *S. cerevisiae* is *RAD6* dependent (8). Thus, N-end rule pathway function is assayed by examining the steady-state level of β-Gal activity in a strain expressing the Arg–β-Gal test protein versus one expressing the Met–β-Gal test protein. pLG-Ub-Pro-βgal expresses ubiquitin–Pro–β-Gal fusion protein, which is not rapidly processed but is degraded via an *RAD6*-independent pathway (2, 24); this test protein therefore provides a control for *RAD6*-independent proteolysis.

To ease the construction of *rad6*Δ strains cotransformed with each of the Met–, Arg–, or Pro–β-Gal test protein-expressing constructs and one of the *RAD6*-expressing constructs, we constructed homozygous *rad6*Δ/*rad6*Δ diploids containing both, as follows. YMW1*rad6*Δ::*LEU2* was transformed with pLG-Ub-Met-βgal, pLG-Ub-Arg-βgal, or pLG-Ub-Pro-βgal (all of which are *URA3* marked). These strains were then mated to YMW2*rad6*Δ::*LEU2* transformed with YCplac22, YCplac22-RAD6 (wild type), or YCplac22-RAD6 scan mutants. N-end rule pathway tester diploids containing both test protein expression vectors and *RAD6*-encoding vectors were then selected by growth on SC-Ura-Trp media.

To assay for relative steady-state β-Gal levels, the diploids were grown overnight in SC-Ura-Trp+raffinose media at 30°C, inoculated into SC-Ura-Trp+galactose media, and grown again at 30°C until an OD_{600} of 1 to 3 was reached. An amount of cells equivalent to 100 μl of culture with an OD_{600} of 1.0 was pelleted, and the cells were resuspended in 0.5 ml of Z buffer (0.1 M $NaPO_4$ [pH 7.0], 10 mM KCl, 1 mM $MgSO_4$, 38 mM 2-mercaptoethanol). A total of 20 μl of chloroform and 10 μl of 0.1% (wt/vol) sodium dodecyl sulfate (SDS) were added to the cells, which were then vortexed for 10 s and preincubated at 30°C for 5 min. A total of 0.1 ml of 4-mg/ml *o*-nitrophenyl-β-D-galactopyranoside (ONPG) was then added, the mixture was incubated for 6 min at 30°C, and the reaction was terminated by the addition of 0.5 ml of 1 M Na_2CO_3. Reaction mixtures were then spun in a microcentrifuge at top speed for several seconds, and the OD_{420} of the supernatant was assayed with a Novaspec spectrophotometer.

Assay for sporulation in *rad6*Δ::*LEU2*/*rad6*Δ::*LEU2* homozygous null mutants. Homozygous *rad6*Δ/*rad6*Δ diploids containing YCplac33, YCplac33-RAD6 (wild type), or YCplac33-RAD6 scan mutant-encoding plasmids were made by mating YMW1 strains transformed with the YCplac33 plasmids with YMW2 transformed with YCplac22; diploids were selected for by growth on SC-Ura-Trp plates. To test for intra-allelic complementation of the sporulation defect of *rad6*Δ/*rad6*Δ strains, diploids were made as described above, except that the YCplac22 vector in YMW2 contained the appropriate *RAD6*-encoding construct. To assay for sporulation, diploids were grown in YPD and then incubated on solid or in liquid sporulation media supplemented with amino acids (1) for several days. The same results were obtained when sporulation was done in liquid or on solid media; the results in Table 1 are from sporulation on solid media. Sporulation was measured as the percentage of total asci relative to asci plus unsporulated cells, by counting at least 200 cells with a hemacytometer.

Expression of RAD6 activity in bacteria. *E. coli* BL21 transformed with wild-type or mutant pET-21(+)-RAD6 expression vectors was grown in Luria broth with 100 μg of ampicillin per ml overnight, and 50 μl of the culture was inoculated into 5 ml of Luria broth with ampicillin and grown for 2 h at 37°C. After 1 ml of culture was removed to assay for uninduced protein expression by SDS-polyacrylamide gel electrophoresis (PAGE), isopropyl-β-D-thiogalactopyranoside (IPTG) was added to the remaining 4 ml to a final concentration of 1 mM to induce RAD6 expression, and growth continued at 37°C for 2 h more. After 1 ml was removed from the induced culture to assay for induced RAD6 expression, the remaining 3 ml of cell culture was pelleted and resuspended in 200 μl of 50 mM Tris-HCl (pH 7.5) containing a final concentration of 1× PIC-D and 1× PIC-W protease inhibitor cocktails (1,000× PIC-D contained 88 mg of

TABLE 1. Summary of *rad6* scan mutants and phenotypes[a]

Designation	Mutation	In vivo phenotype				In vitro activity	
		N-end rule pathway function[b]	Temp resistance[c]	Sporulation[d] (%)	Resistance to UV[e]	Ub-thiol ester formation	Ub conjugation to histones
V	*rad6*::*LEU2* (null)	−	Ts Cs	− (0)	−	NA[f]	NA
A	6, 7, 8A	−	Ts Cs	− (0)	−	+	+
F	71, 75A	ND[g]	Ts Cs	ND	−	+	+
G	86, 90A	−	Ts Cs	− (0)	+	+	−
D	49, 50A	−	Ts Cs	− (0)	++	+	+
B	11, 14, 15A	−	+	+ (54)	++	+	+
C	17, 18, 19A	+	+	+ (57)	+++	+	ND
E	58, 60, 61, 62A	+	+	+ (61)	+++	−	ND
H	131, 132, 134A	+	+	+ (65)	+++	+	ND
I	139, 140, 142, 143A	+	+	+ (67)	+++	+	ND
W	*RAD6* (wild type)	+	+	+ (67)	+++	+	+

[a] *RAD6* scan mutants are arranged to illustrate the nesting of their phenotypes. Ub, ubiquitin.
[b] Designations used to describe N-end rule pathway function are as follows: +, wild-type N-end rule pathway function as judged by Arg–β-Gal steady-state levels; −, deficiency in N-end rule pathway function as judged by a steady-state level of Arg–β-Gal that was greater than 50% of the steady-state level of Met–β-Gal.
[c] Ts, temperature sensitive; Cs, cold sensitive; +, temperature resistant.
[d] Sporulation efficiency of homozygous *rad6*Δ/*rad6*Δ diploids transformed with *RAD6* scan mutants. The numbers in parentheses are the percentages of asci formed.
[e] Designations used to describe UV sensitivity are as follows: −, no growth observed after 5 J of UV per m^2; +, growth observed after 5 J of UV per m^2 but not after 30 J of UV per m^2; ++, growth observed up to at least 15 J of UV per m^2; +++, good growth observed at up to 30 J of UV per m^2 per min (wild-type resistance).
[f] NA, not applicable.
[g] ND, not determined.

phenylmethylsulfonyl fluoride [0.5 M] per ml, 5 mg of pepstatin A per ml, 1 mg of chymostatin per ml, 1.1 mg of phosphoramidon per ml, and 7.2 mg of E-64 per ml, all dissolved in dimethyl sulfoxide; 1,000× PIC-W contained 208 mg of benzamidine [1 M] per ml, 131 mg of aminocaproic acid [1 M] per ml, 5 mg of aprotinin per ml, 1 mg of leupeptin per ml, and 190 mg of sodium metabisulfite [1 M] per ml, all dissolved in water). Cells were lysed by sonication. The lysate was centrifuged at 4°C for 30 min at 16,000 × *g*, and equal amounts of total protein from the supernatant were used for assay of E2 activity. Protein concentrations of bacterial lysates were measured by the Bradford assay; the typical lysate concentration was about 20 mg/ml. We were unable to visualize expressed RAD6 polypeptide by SDS-PAGE of cell lysates, although RAD6 protein activity (thioester formation with ubiquitin and conjugation of ubiquitin onto histones) was easily detected for all RAD6 constructs except for mutant E. This is likely because our constructs have not been optimized for expression in *E. coli*; in particular, expression of RAD6 protein in bacteria depends on a cryptic ribosome binding site contained within the *Eco*RI-*Eco*RI RAD6 insert that, while functional, is not set at the expected optimum distance from the RAD6-initiating ATG codon.

In vitro assay for RAD6 ubiquitin-conjugating enzyme activity. To assay for ubiquitin conjugation, reaction mixtures (20 μl) contained final concentrations of 50 mM Tris-HCl (pH 7.5), 5 mM $MgCl_2$, 2 mM ATP, 50 mM KCl, and 0.2 mM dithiothreitol and (when present) 500 ng of purified yeast E1, 85 μg of *E. coli* extract, 10 μg of histone H2B, and 550 ng of ^{125}I-ubiquitin (labeled by the chloramine T method). Ubiquitin-activating (E1) enzyme was purified from *S. cerevisiae* essentially as previously described (22), except that yeast lysate was prepared from dried 90% active viable *S. cerevisiae* type II (Sigma; catalog number YSC-2) by a procedure to be described elsewhere. The reaction mixtures were incubated at the indicated temperature for 30 min and then 10 μl of stop buffer (200 mM Tris-HCl [pH 6.8], 6% [wt/vol] SDS, 30% [vol/vol] glycerol, 15% [vol/vol] 2-mercaptoethanol, 0.06% [wt/vol] bromophenol blue) was added and incubated at 100°C for 3 min. Samples were electrophoresed by SDS–12.5% PAGE and then autoradiographed with Amersham HR film. Thioester bond formation between ubiquitin and RAD6 was detected in identical reaction mixtures lacking histone H2B; for these assays the stop buffer did not contain 2-mercaptoethanol and the samples were electrophoresed without prior boiling.

RESULTS AND DISCUSSION

We wished to identify *RAD6* (*UBC2*) N-terminal domain mutants which are enzymatically active as judged by competence for unfacilitated (E3-independent) E2 activity but which are nevertheless unable to support RAD6-dependent functions in vivo. Because it seemed likely that the majority of randomly obtained mutations would catalytically inactivate the E2 enzyme (for example, by causing the protein to misfold), we used a directed mutagenesis strategy to search for mutants with the desired properties.

Specifically, we examined the feasibility of obtaining such mutants by charge-to-alanine scanning mutagenesis. In this approach, discrete clusters of charged residues (Asp, Glu, Arg, or Lys) are mutated to alanine (9, 12, 39). Such mutations may disrupt protein-protein interactions while causing only a minor perturbation in protein structure. This strategy has been used to obtain conditional alleles of genes (such as actin) which had yielded few such mutants by untargeted mutagenesis (39). The *RAD6* scan mutants described here consisted of mutations to Ala of all charged residues when two or more fell within a moving window of five. A total of nine *RAD6* scan mutants were constructed (Table 1; Fig. 1). We refer to each mutant by the letter designation given in Table 1. The scan mutants were cloned into both low-copy-number *URA3*-marked vectors (YCplac33) and low-copy-number *TRP1*-marked vectors (YCplac22)

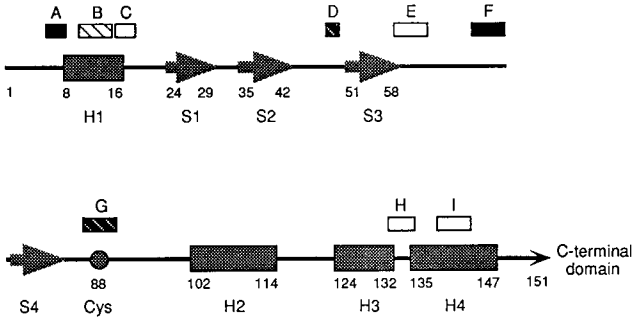

FIG. 1. Location of *RAD6* scan mutants relative to putative RAD6 protein secondary structure. The assignment of secondary structural elements is based on a comparison of the *RAD6* and *A. thaliana UBC1* sequences and the X-ray crystallographic structure of the UBC1 protein (7). The four putative α-helices (H1 through H4) are denoted by rectangles; the four putative β-strands (S1 through S4) are denoted by large arrows. The active-site cysteine at residue 88 is also indicated. The residue numbers at the start and end of the various structural elements are noted just below their representation. The regions of the RAD6 protein spanned by the scan mutants A through I are indicated by the rectangles positioned over the representation of the RAD6 putative secondary structure. The density of cross-hatching within the rectangles reflects the severity of the in vivo defect shown by the scan mutants ranging from wild-type behavior (no cross-hatching) to severely dysfunctional (solid). See text for details regarding the specifics of the in vivo phenotypes displayed by the mutants.

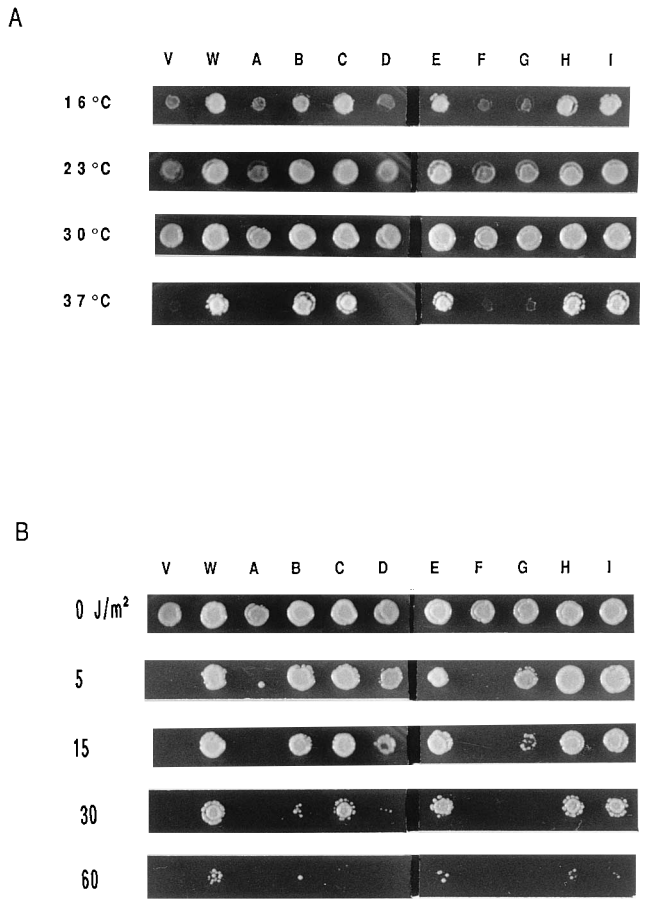

FIG. 2. Complementation of temperature-sensitive growth and UV sensitivity by *RAD6* scan mutants. (A) YMW1*rad6*Δ::*LEU2* transformed with YCplac33 (vector only [V]), YCplac33-RAD6 (wild type [W]) or YCplac33 encoding *RAD6* scan mutant A through I was stamped onto SC-Ura media as described in Materials and Methods and incubated at the indicated temperature prior to photography. (B) YMW1*rad6*Δ::*LEU2* transformed with the same set of YC plac33-based plasmids as in panel A was stamped onto SC-Ura media, irradiated with germicidal UV at the indicated dosages, and grown at 30°C (as described in Materials and Methods) prior to photography.

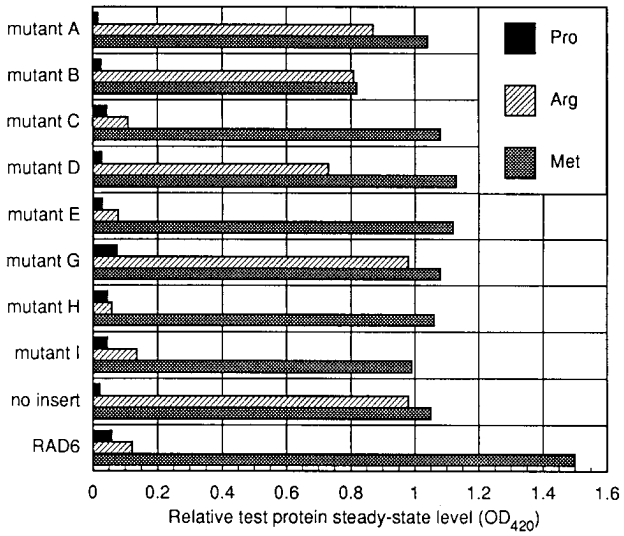

FIG. 3. Complementation of N-end rule pathway function by *RAD6* scan mutants. N-end rule pathway function was assayed by measurement of β-Gal test protein steady-state levels. The bars denote relative β-Gal steady-state levels in diploid tester strains expressing ubiquitin–X–β-Gal test proteins. Thus, failure of a *RAD6* mutant to support N-end rule pathway function is indicated by a steady-state level of Arg–β-Gal that approaches that of Met–β-Gal.

and then transformed into the appropriate *rad6*Δ::*LEU2* disruption strains for testing.

We tested the *RAD6* scan mutants for complementation of four *RAD6*-associated phenotypes: (i) temperature sensitivity of growth (Fig. 2A); (ii) sensitivity to UV (Fig. 2B); (iii) loss of N-end rule pathway function (Fig. 3); and (iv) failure of homozygous *rad6*Δ/*rad6*Δ diploids to sporulate (Table 1). Details on how different phenotypes were assayed are described in Materials and Methods.

In general, different scan mutants displayed different spectra of phenotypic defects. Mutant A, which mutated a set of three consecutive Arg residues near the N terminus to Ala, was the most severely affected; the phenotype of a *rad6*Δ::*LEU2* yeast strain carrying mutant A on a low-copy-number plasmid was indistinguishable from that of a *rad6* null mutant. Mutant F was as severely affected with respect to temperature resistance and UV resistance, but other phenotypes were not tested. On the other hand, several other scan mutants (C, E, H, and I) were virtually indistinguishable from wild-type *RAD6*. The remaining scan mutants showed intermediate degrees of compromised function. Interestingly, a review of the phenotypes displayed by the scan mutants (Table 1) suggests that the mutant phenotypes were nested. Mutants D and G were defective in N-end rule pathway function, temperature sensitive, and deficient in sporulation but were partially resistant to UV. Mutant B was defective in N-end rule pathway function but was nearly wild type with respect to temperature resistance and sporulation and only slightly sensitive to UV. An examination of Table 1 gives the impression that, among those functions tested, N-end rule-dependent proteolysis was the most easily perturbed by the scan mutations, followed by temperature or cold resistance and sporulation (which were correlated) and resistance to UV.

Previously described *RAD6* mutations also show differential inactivation of specific functions. A mutation which deletes all of the RAD6 C-terminal polyacidic tail yields an allele which complements the UV sensitivity of a *rad6* null mutant but is deficient in sporulation and N-end rule pathway function (28, 29, 38). On the other hand, a mutant allele which encodes a *RAD6* lacking its first nine residues (*rad6*Δ_{1-9}) is unable to complement the sporulation defect or loss of N-end rule pathway function of a *rad6* null mutant and is significantly more UV sensitive than the wild type. However, UV mutagenesis in a *rad6* deletion strain overexpressing plasmid-encoded *rad6*Δ_{1-9} is even higher than in a wild-type strain (38). Our *RAD6* scan mutant A targets a triplet of Arg residues that lie in the nine-residue segment that is deleted in *rad6*Δ_{1-9} and yields as extreme a mutant phenotype with respect to the functions we tested as did *rad6*Δ_{1-9}.

For several *RAD6*-dependent functions such as resistance to DNA-damaging agents, sporulation, and temperature sensitivity, little is known about the identity or even the number of the relevant substrates. In particular, we could not exclude the possibilities that a particular function (such as sporulation) required the targeting of several substrates and that different scan mutants failed to support that function because they failed to target distinct and separate substrates. We reasoned that if this was the case, we might observe intra-allelic complementation between different scan mutants that were defective in nonoverlapping subsets of essential targets. Therefore, we

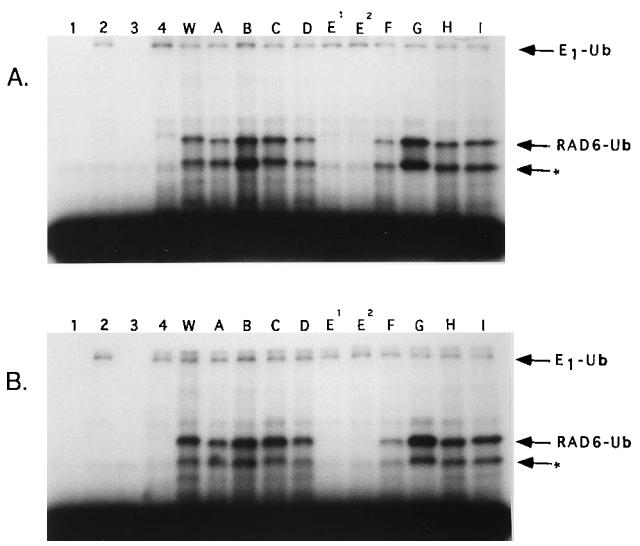

FIG. 4. Ubiquitin-thiol ester-forming activity of RAD6 wild-type and scan mutant proteins expressed in *E. coli*. The proteins tested were wild-type RAD6 (W) and single-scan mutants A through I. Lanes 1 through 4 show the results of control reactions with (lane 2 and 4) or without (lanes 1 and 3) added E1 and with (lanes 3 and 4) or without (lanes 1 and 2) extract from bacteria transformed with the pET21-(+) vector only (no RAD6). Reactions were performed at either 30°C (A) or 37°C (B). The pattern obtained from the control reactions (lanes 1 through 4) was essentially identical to the pattern found in other control reactions which omitted ATP or ubiquitin-activating enzyme, except for the presence of the high-molecular-weight E1-ubiquitin thioester under nonreducing conditions. The lower-molecular-weight band denoted by an asterisk is most likely derived from proteolysis of the expressed RAD6 protein, probably by proteolysis of its acidic C-terminal tail.

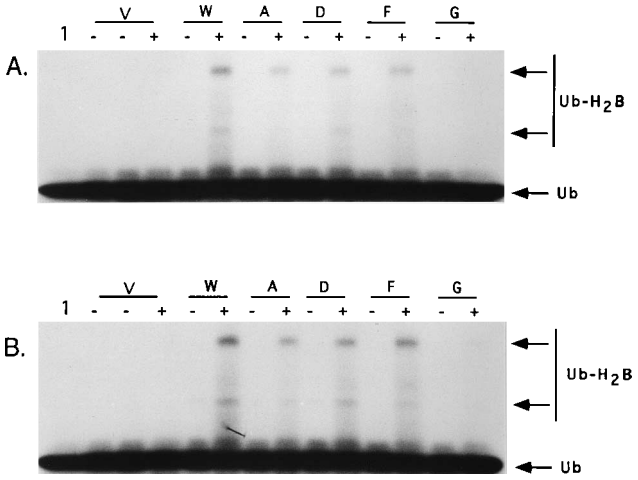

FIG. 5. Ubiquitin conjugation activity of RAD6 wild-type and single-scan mutant proteins expressed in *E. coli*. The proteins tested were those encoded by wild-type *RAD6* (W) and single-scan mutants A, D, F, and G. Reactions were performed at either 30°C (A) or 37°C (B) in either the absence (−) or presence (+) of histones. Lanes 1, control reaction done in the absence of bacterial extract; lanes V, control reactions done using extract from bacteria transformed with the pET21-(+) vector only (no RAD6; a minus-histone control reaction [denoted by −] was run in duplicate). The patterns obtained from the control reactions (lanes 1 and V) were identical to the patterns found in control reactions which omitted either ATP or ubiquitin-activating enzyme.

tested for intra-allelic complementation of a subset of *RAD6* scan mutants that were defective with respect to temperature sensitivity, resistance to UV, or sporulation. To do this, we constructed homozygous *rad6*Δ/*rad6*Δ diploids transformed with two distinct scan mutants (specifically, mutants A, D, and G carried on YCplac22 or YCplac33, as well as wild-type *RAD6* and vector-only controls). In no case did we observe intra-allelic complementation (data not shown). We also verified that all *RAD6* scan mutant phenotypes were recessive to wild-type *RAD6* (data not shown).

The phenotype of the most severely affected scan mutations could be trivially explained if the scan mutation eliminated the enzymatic (unfacilitated) activity of the RAD6 polypeptide. To address this possibility, *RAD6* scan mutations were cloned into a T7 expression vector and expressed in *E. coli*. Extract from *E. coli* containing the RAD6 proteins was tested for (i) thiol ester formation with ubiquitin and (ii) conjugation of ubiquitin onto histones. Although we could not detect the expressed RAD6 protein by examination of Coomassie blue-stained SDS-polyacrylamide gels of *E. coli* extract, we could readily detect E2 activity in the crude extracts (Fig. 4). Indeed, all *RAD6* scan mutant proteins formed a thiol ester with ^{125}I-labeled ubiquitin except for mutant E. Protein expressed from *RAD6* scan mutants A, D, and F showed conjugating activity with respect to histone ubiquitination at both 30 and 37°C (Fig. 5). Mutant G, however, displayed a strong defect in histone ubiquitination (though not thioester formation) relative to that of the other proteins examined; this is not surprising, since the amino acid changes in mutation G (changes to alanine at positions 86 and 89 [86, 89A] [Table 1]) straddle the active-site cysteine at residue 88. Thus, three of four of the mutants most severely affected with respect to in vivo function still encode protein that is competent for some unfacilitated (E3-independent) ubiquitination in vitro. We do not yet understand our failure to detect in vitro activity for mutant E, which in fact behaves almost identically to wild-type *RAD6* with respect to in vivo activity (Table 1). We examined both the in vivo phenotypes and in vitro activities for two independently obtained isolates of mutant E, and both behaved identically. We cannot yet exclude the possibility that mutant E is simply more poorly expressed in *E. coli* than the other *RAD6* scan mutants. Because we could not detect ubiquitin-thioester formation with mutant E, we did not assay it for ubiquitination of histone H2B.

We cannot rigorously rule out that some of the severe defects we observe for some mutants are not due to a defect in enzymatic efficiency in vivo. Time courses of ubiquitination reactions with mutant RAD6 protein suggests that mutations A, D, and F are only slightly less efficient catalytically than wild-type RAD6 protein (data not shown), but an examination of purified mutant activities is needed for a more detailed, quantitative comparison of wild-type versus mutant E2 activity. Nevertheless, given the ease with which we can observe E2 activity in vitro, we suggest that the in vivo defects of our *RAD6* scan mutations are not due to a gross defect in their enzymatic function (say, caused by misfolding of the enzyme). Instead, we suggest that the scan mutations might act by disrupting interactions between *RAD6* and *trans*-acting factors that govern either its activity or its substrate selectivity (such as E3s). Their nuclear localization (38) may also be perturbed. However, the deletion of the first nine residues of RAD6 does not affect its nuclear localization (38), and thus mutation A at least should be appropriately localized. The nested behavior of phenotypes may reflect differing minimum requirements for *RAD6* activity for execution of *RAD6*-dependent functions. In other words, less *RAD6* activity may be required for DNA repair than is required for N-end rule pathway function. Alternatively, it may reflect that the relevant complexes formed by *RAD6* and associated factors needed for one function are more easily per-

turbed than those required for another. Differential sensitivity of binding to cofactors has been observed for the rad6Δ_{1-9} mutant protein, which forms complexes with the RAD18 protein but not with UBR1 (the E3 required for N-end rule pathway function [4]). Again, more detailed enzymological characterization of the more severely affected mutants will be needed to address these issues.

While the crystal structure for yeast RAD6 has not been determined, that of the homologous UBC1 from *Arabadopsis thaliana* (7) allows us to examine the severity of the scan mutant phenotypes as a function of their likely locations in RAD6. As expected, all of the scan mutants appear to target surface residues. However, the scan mutants with the most severe phenotypes (mutants A, F, G, and D) in general do not cluster in the RAD6 structure but rather appear to target distinct regions of the protein (with the exception of mutants F and G, which lie adjacent to one another near the active site). Mutant D in particular targets two residues that lie on a narrow edge of the enzyme, on a side opposite from the active site. In contrast, mutants A, B, and C, which range in phenotype from the most severe (mutant A) to weak (mutant B), and to the wild type (mutant C), are not only adjacent with respect to linear sequence but are also adjacent to one another with respect to the protein itself, clustering near the N terminus (data not shown).

To summarize, our results indicate that charge-to-alanine scanning mutagenesis is a viable strategy for obtaining novel mutant E2s. With *RAD6*, the majority of mutants appeared to retain at least some unfacilitated (E3-independent) activity, even though they were defective for specific in vivo functions. Such mutants are qualitatively different from ones that are wholly deficient in E2 catalytic activity or are misfolded and should be useful for identifying and characterizing interacting proteins by both genetic and biochemical approaches.

ACKNOWLEDGMENTS

We thank Patricia Birgeneau and Blondell Brown for technical assistance and Mark Solomon and Zach Pitluk for comments.

This work was supported by grant CB-80 from the American Cancer Society. D.K.G. is a Scholar of the Leukemia Society of America.

REFERENCES

1. **Ausubel, F. M., R. Brent, R. E. Kingston, D. D. Moore, J. G. Seidman, J. A. Smith, and K. Struhl (ed.).** 1991. Current protocols in molecular biology, vol. 2. John Wiley & Sons, Inc., New York.
2. **Bachmair, A., D. Finley, and A. Varshavsky.** 1986. In vivo half-life of a protein is a function of its amino-terminal residue. Science **234:**179–186.
3. **Bachmair, A., and A. Varshavsky.** 1989. The degradation signal in a short-lived protein. Cell **56:**1019–1032.
4. **Bailly, V., J. Lamb, P. Sung, S. Prakash, and L. Prakash.** 1994. Specific complex formation between RAD6 and RAD18 proteins: a potential mechanism for targeting RAD6 ubiquitin-conjugating activity to DNA damage sites. Genes Dev. **8:**811–820.
5. **Balzi, E., M. Choder, W. Chen, A. Varshavsky, and A. Goffeau.** 1990. Cloning and functional analysis of the arginyl-tRNA-protein transferase gene ATE1 of Saccharomyces cerevisiae. J. Biol. Chem. **265:**7464–7471.
6. **Bartel, B., I. Wunning, and A. Varshavsky.** 1990. The recognition component of the N-end rule pathway. EMBO J. **9:**3179–3189.
7. **Cook, W. J., L. C. Jeffrey, M. L. Sullivan, and R. D. Vierstra.** 1992. Three-dimensional structure of a ubiquitin-conjugating enzyme (E2). J. Biol. Chem. **267:**15116–15121.
8. **Dohmen, R. J., K. Madura, B. Bartel, and A. Varshavsky.** 1991. The N-end rule is mediated by the UBC2(RAD6) ubiquitin-conjugating enzyme. Proc. Natl. Acad. Sci. USA **88:**7351–7355.
9. **Ducommun, B., P. Brambilla, and G. Draetta.** 1991. Mutations at sites involved in Suc1 binding inactivate Cdc2. Mol. Cell. Biol. **11:**6177–6184.
10. **Ellison, K. S., T. Gwozd, J. A. Prendergast, M. C. Paterson, and M. J. Ellison.** 1991. A site-directed approach for constructing temperature-sensitive ubiquitin-conjugating enzymes reveals a cell cycle function and growth function for RAD6. J. Biol. Chem. **266:**24116–24120.
11. **Finley, D., and V. Chau.** 1991. Ubiquitination. Annu. Rev. Cell Biol. **7:**25–69.
12. **Gibbs, C. S., and M. J. Zoller.** 1991. Rational scanning mutagenesis of a protein kinase identifies functional regions involved in catalysis and substrate interactions. J. Biol. Chem. **266:**8923–8931.
13. **Gietz, R. D., and A. Sugino.** 1988. New yeast-Escherichia coli shuttle vectors constructed with in vitro mutagenized yeast genes lacking six-base pair restriction sites. Gene **74:**527–534.
14. **Gonda, D. K.** 1994. Molecular genetics of the ubiquitin system, p. 23–51. *In* A. Schwartz and A. Ciechanover (ed.), Cellular proteolytic systems. Wiley-Liss, New York.
15. **Gonda, D. K., A. Bachmair, I. Wunning, J. W. Tobias, W. S. Lane, and A. Varshavsky.** 1989. Universality and structure of the N-end rule. J. Biol. Chem. **264:**16700–16712.
16. **Heller, H., and A. Hershko.** 1990. A ubiquitin-protein ligase specific for type III protein substrates. J. Biol. Chem. **265:**6532–6535.
17. **Hershko, A., and A. Ciechanover.** 1992. The ubiquitin system for protein degradation. Annu. Rev. Biochem. **61:**761–807.
18. **Hershko, A., H. Heller, S. Elias, and A. Ciechanover.** 1983. Components of ubiquitin-protein ligase system. Resolution, affinity purification, and role in protein breakdown. J. Biol. Chem. **258:**8206–8214.
19. **Hershko, A., H. Heller, E. Eytan, and Y. Reiss.** 1986. The protein substrate binding site of the ubiquitin-protein ligase system. J. Biol. Chem. **261:**11992–11999.
20. **Higuchi, R.** 1989. Using PCR to engineer DNA, p. 61–70. *In* H. A. Erlich, (ed.), PCR technology. Stockton Press, New York.
21. **Jentsch, S.** 1992. The ubiquitin-conjugation system. Annu. Rev. Genet. **26:**179–207.
22. **Jentsch, S., J. P. McGrath, and A. Varshavsky.** 1987. The yeast DNA repair gene RAD6 encodes a ubiquitin-conjugating enzyme. Nature (London) **329:**131–134.
23. **Jentsch, S., W. Seufert, and H. P. Hauser.** 1991. Genetic analysis of the ubiquitin system. Biochim. Biophys. Acta **1089:**127–139.
24. **Johnson, E. S., B. Bartel, W. Seufert, and A. Varshavsky.** 1992. Ubiquitin as a degradation signal. EMBO J. **11:**497–505.
25. **Kolman, C. J., J. Toth, and D. K. Gonda.** 1992. Identification of a portable determinant of cell cycle function within the carboxyl-terminal domain of the yeast CDC34 (UBC3) ubiquitin conjugating (E2) enzyme. EMBO J. **11:**3081–3090.
26. **Lawrence, C. W., T. O'Brien, and J. Bond.** 1984. UV-induced reversion of his4 frameshift mutations in rad6, rev1, and rev3 mutants of yeast. Mol. Gen. Genet. **195:**487–490.
27. **Liebman, S. W., and G. Newnam.** 1993. A ubiquitin-conjugating enzyme, RAD6, affects the distribution of Ty1 retrotransposon integration positions. Genetics **133:**499–508.
28. **Madura, K., R. J. Dohmen, and A. Varshavsky.** 1993. N-recognin/Ubc2 interactions in the N-end rule pathway. J. Biol. Chem. **268:**12046–12054.
29. **Morrison, A., E. J. Miller, and L. Prakash.** 1988. Domain structure and functional analysis of the carboxyl-terminal polyacidic sequence of the RAD6 protein of *Saccharomyces cerevisiae*. Mol. Cell. Biol. **8:**1179–1185.
30. **Prakash, L.** 1981. Characterization of postreplication repair in Saccharomyces cerevisiae and effects of rad6, rad18, rev3 and rad52 mutations. Mol. Gen. Genet. **184:**471–478.
31. **Prakash, S., P. Sung, and L. Prakash.** 1993. DNA repair genes and proteins of Saccharomyces cerevisiae. Annu. Rev. Genet. **27:**33–70.
32. **Reiss, Y., H. Heller, and A. Hershko.** 1989. Binding sites of ubiquitin-protein ligase. Binding of ubiquitin-protein conjugates and of ubiquitin-carrier protein. J. Biol. Chem. **264:**10378–10383.
33. **Schiestl, R. H., and R. D. Gietz.** 1989. High efficiency transformation of intact yeast cells using single stranded nucleic acids as a carrier. Curr. Genet. **16:**339–346.
34. **Sung, P., E. Berleth, C. Pickart, S. Prakash, and L. Prakash.** 1991. Yeast RAD6 encoded ubiquitin conjugating enzyme mediates protein degradation dependent on the N-end recognizing E3 enzyme. EMBO J. **10:**2187–2193.
35. **Sung, P., S. Prakash, and L. Prakash.** 1988. The RAD6 protein of Saccharomyces cerevisiae polyubiquitinates histones, and its acidic domain mediates this activity. Genes Dev. **2:**1476–1485.
36. **Sung, P., S. Prakash, and L. Prakash.** 1990. Mutation of cysteine-88 in the Saccharomyces cerevisiae RAD6 protein abolishes its ubiquitin-conjugating activity and its various biological functions. Proc. Natl. Acad. Sci. USA **87:**2695–2699.
37. **Sung, P., S. Prakash, and L. Prakash.** 1991. Stable ester conjugate between the Saccharomyces cerevisiae RAD6 protein and ubiquitin has no biological activity. J. Mol. Biol. **221:**745–749.
38. **Watkins, J. F., P. Sung, S. Prakash, and L. Prakash.** 1993. The extremely conserved amino terminus of RAD6 ubiquitin-conjugating enzyme is essential for amino-end-rule-dependent protein degradation. Genes Dev. **7:**250–261.
39. **Wertman, K. F., D. G. Drubin, and D. Botstein.** 1992. Systematic mutational analysis of the yeast ACT1 gene. Genetics **132:**337–350.